PROCEEDINGS OF SCIENCE

Search for single top quark production at the Tevatron

Michael Begel*
University of Rochester (USA)
E-mail: begel@fnal.gov
On behalf of the CDF & DØ collaborations

We review the status of the search for the electroweak production of single top quarks by the CDF and DØ collaborations at the Fermilab Tevatron Collider. Neither experiment finds evidence for single top quark production and they therefore set 95% C.L. upper limits on the production cross section. The CDF limits, with 160 pb^{-1}, are 10.1 pb for the t channel, 13.6 pb for the s channel, and 17.8 pb for the combination of the s and t channels. The DØ limits are 4.4 pb for the t channel and 5.0 pb for the s channel in 370 pb^{-1}.

International Workshop on Top Quark Physics
January 12-15, 2006
Coimbra, Portugal

*Speaker.

PoS(TOP2006)012

The top quark, discovered in 1995 by the CDF and DØcollaborations at the Fermilab Tevatron Collider [1], is the heaviest fundamental particle with a mass $m_{\rm top} = 172.5 \pm 2.9$ GeV [2]. Studies of top-quark production probe aspects of the strong and electroweak sectors of the Standard Model and have the potential for the discovery of physics beyond the Standard Model. While top quarks are primarily produced in pairs through the strong interaction, individual top quarks may be produced via the electroweak interaction. Measurements of single top-quark production access the CKM matrix element $|V_{tb}|$ and properties of the tWb vertex. The two dominant signal channels for single top-quark production at the Tevatron are displayed in Fig. 1. The Standard Model expectation [3] for single top-quark production in $p\bar{p}$ interactions at $\sqrt{s} = 1.96$ TeV is 0.88 ± 0.11 pb in the s channel and 1.98 ± 0.25 pb in the t channel (assuming $m_{\rm top} = 175$ GeV). By comparison, the cross section for the production of pairs of top quarks is 6.77 ± 0.42 pb [4].

The top quark decays predominantly to a W boson and a b quark. The final state for the s channel therefore consists of the W boson decay products and two b quarks. Likewise, the t channel final state has the W boson decay products and a b quark from the top quark decay, along with a forward b quark and a light quark. Higher-order processes can result in additional jets. The analyses described herein only considered events where the W boson decay resulted in a high-p_T electron or muon. The jet associated with the b quark was identified by the presence of a displaced secondary vertex. The criteria used by each collaboration to select single top-quark candidate events are summarized in Table 1. These requirements were chosen to maximize signal acceptance while minimizing background contributions.

CDF used MADEVENT [5] to generate events with single top quarks while DØused COMPHEP [6]. The outputs of both generators were passed through PYTHIA [7] for radiation and hadronization and through the full detector simulations. In both cases, the b quark p_T distribution in the t channel was adjusted to match the next-to-leading order prediction. The dominant backgrounds to single top-quark production include $t\bar{t}$, $Wb\bar{b}$, and QCD multi-jet events. PYTHIA was used for $t\bar{t}$ production by CDF and ALPGEN [8] by DØ ALPGEN was used by both collaborations for the Wjj, Wcj, Wcc, and $Wb\bar{b}$ background distributions. Instrumental and multi-jet backgrounds were determined from the data. The electron and muon data in the single and double

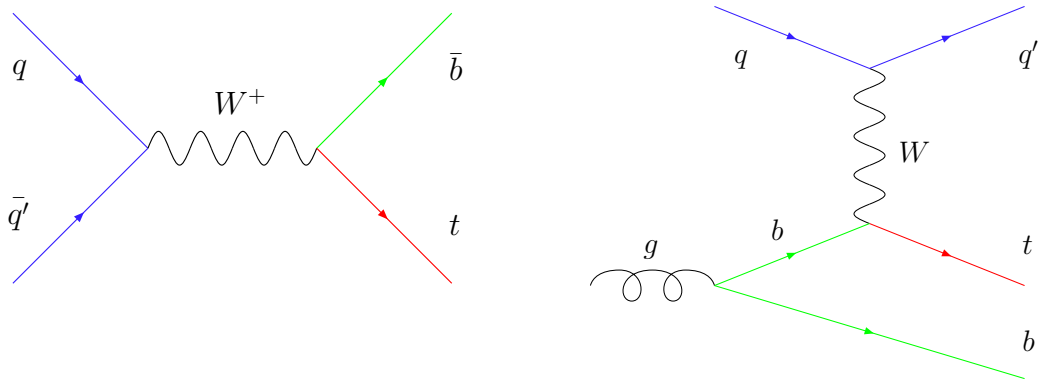

Figure 1: Representative Feynman diagrams for single top quark production. An s-channel diagram is on the left; a t-channel diagram is on the right.

Object	CDF	DØ
Lepton	e $p_T > 20$ GeV $\lvert\eta\rvert < 1$ μ $p_T > 20$ GeV $\lvert\eta\rvert < 1$	e $p_T > 15$ GeV $\lvert\eta\rvert < 1.1$ μ $p_T > 15$ GeV $\lvert\eta\rvert < 2.0$
Neutrino	$\not\!\!E_T > 20$ GeV	$\not\!\!E_T > 15$ GeV
Jets	exactly 2 $p_T > 15$ GeV $\lvert\eta\rvert < 2.8$	$2 \leq N_{\text{jets}} \leq 4$ $p_T > 15$ GeV $\lvert\eta\rvert < 3.4$ leading jet $p_T > 25$ GeV and $\lvert\eta\rvert < 2.5$
b tag	≥ 1 (leading jet $p_T > 30$ GeV in 1 b-tag channel)	≥ 1 (require at least one untagged jet for t channel)
Mass cut	$140 < M_{\ell\nu b} < 210$ GeV $76 < M_{\ell\ell} < 106$ GeV	
Acceptance s Acceptance t	$(1.06 \pm 0.08)\%$ $(0.89 \pm 0.07)\%$	$(2.7 \pm 0.2)\%$ $(1.9 \pm 0.2)\%$

Table 1: Summary of event selection criteria used by CDF and DØ.

b-tagged samples were considered separately for the s- and t-channel analyses. The full analyses are described in detail in Refs. [9] and [10].

Correlations between kinematic quantities can be exploited to enhance the discrimination between signal and background. For example, the distribution of the lepton charge Q multiplied by the pseudorapidity η of the untagged jet is asymmetric and peaked forward for the t-channel process while it is mostly symmetric and central for the backgrounds (Fig. 2 (left)). CDF performed a maximum-likelihood fit to this discriminant to estimate the signal content of the data in a 162 pb^{-1} sample (Fig. 2 (right)). This resulted in a 95% C.L. upper limit in the t channel of 10.1 pb with an expectation of 11.2 pb. A limit was placed on the s-channel process of 13.6 pb (12.1 pb expected) through a counting experiment in the double b-tagged sample. The systematic uncertainties associated with these limits are detailed in Table 2. CDF also used the $H_T = \sum p_T$ distribution to

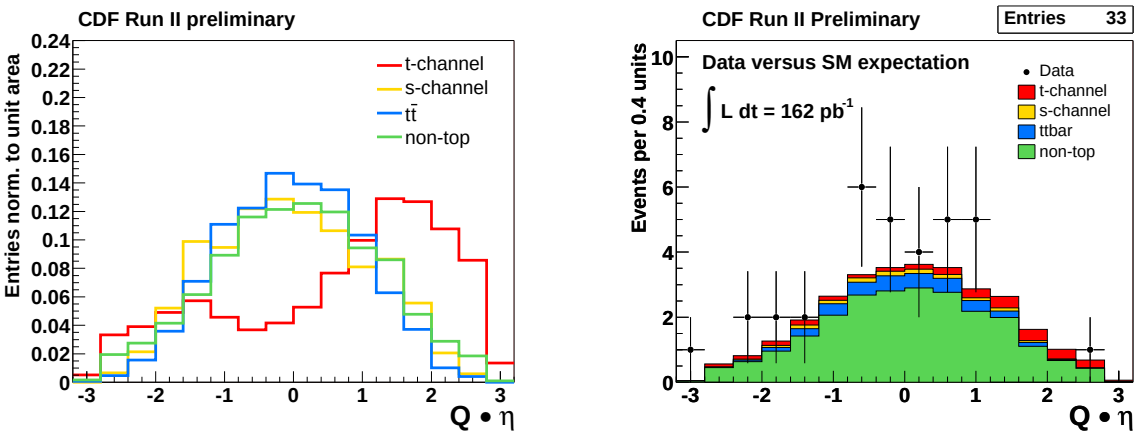

Figure 2: Left: Templates for the single top quark and background processes in the $Q \times \eta$ distribution. Right: Result of the template fit to the CDF single b-tagged data sample for the t channel search.

Source	t channel	s channel	combined
Jet Energy Scale	$^{+2.4}_{-6.7}$	$^{+0.4}_{-3.1}$	$^{+0.1}_{-4.3}$
Initial-State Radiation	± 1.0	± 0.6	± 1.0
Final-State Radiation	± 2.2	± 5.3	± 2.6
PDF	± 4.4	± 2.5	± 3.8
Generator	± 5	± 2	± 3
m_{top}	$^{+0.7}_{-6.9}$	-2.3	-4.4
$\varepsilon_{\text{trigger}}$, ε_{ID}, $\mathscr{L}$	± 9.8	± 9.8	± 9.8

Table 2: Fractional changes in the CDF event efficiency for single top processes in percent. $\varepsilon_{\text{trigger}}$ is the trigger efficiency, ε_{ID} is the lepton identification efficency.

discriminate between single top-quark production and background. While the H_T distribution for the s- and t-channel processes are quite similar, they are somewhat different than those for $t\bar{t}$ or non-top processes (Fig. 3 (left)). A fit of these templates to the data (Fig. 3 (right)) yielded a limit for the combined s- and t-channel single top-quark production of 17.8 pb (13.6 pb expected).

Additional correlations can also be considered. DØapplied a multi-variate statistical approach to search for single top-quark production. Some 25 quantities, including $Q \times \eta$, H_T, masses, momenta, and angles, were input into a neural network to discriminate between the s- and t-channel processes, $t\bar{t}$, and $Wb\bar{b}$. Two of these variables are displayed in Fig. 4. The neural networks were trained on each sample with special care taken to avoid over-training. DØperformed a binned likelihood calculation on the neural network output to set limits on the observation of single-top quark production in a 230 pb^{-1} data sample (Fig. 5). The 95% C.L. limit in the s channel was 6.4 pb (4.5 pb expected) and 5.0 pb (5.8 pb expected) in the t channel. Systematic uncertainties associated with this analysis are summarized in Table 3. A similar multi-variate analysis using decision trees [11] was also pursued by DØwith the 230 pb $^{-1}$ data sample. The 95% C.L. limit was 8.3 pb (4.5 pb expected) in the s channel and 8.1 pb (6.4 pb expected) in the t channel.

A third multi-variate analysis with likelihood discriminants was used by DØto search for

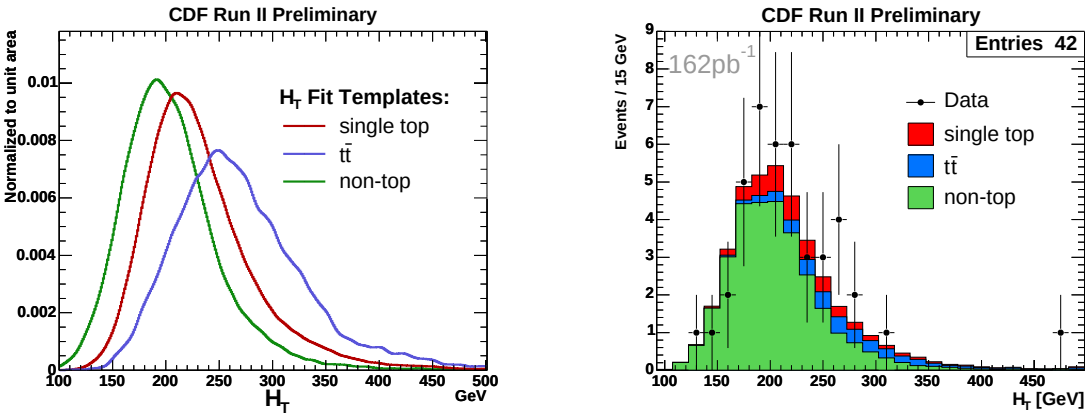

Figure 3: Left: Templates for the single top quark and background processes in the H_T distribution. Right: Result of the template fit to the CDF single b-tagged data sample for the combined search.

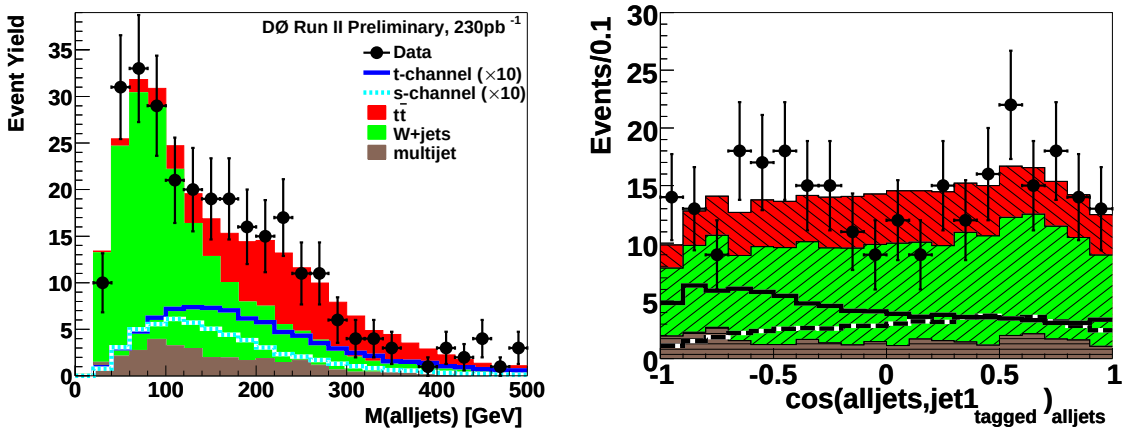

Figure 4: Comparison of signal ($\times 10$), backgrounds, and data with at least one b-tagged jet. Left: invariant mass of all jets. Right: cosine of the angle between the leading *b*-tagged jet and all jets in the all jets rest frame.

single top-quark production in a 370 pb^{-1} data sample. This analysis followed a similar strategy to the neural network analysis described above, but used only the 12 most discriminating variables. The likelihood-filter outputs for signal and background are shown in Fig. 6 for events with two *b*-tagged jets. The number of observed events was consistent with the number of expected events, so DØplaced a 95% C.L. limit of 5.0 pb (3.3 pb expected) in the *s* channel and 4.4 pb (4.3 pb expected) in the *t* channel.

The electroweak production of single top quarks has not yet been observed. Limits have been placed on this production of 5.0 pb in the *s* channel and 4.4 pb in the *t* channel. Although single top-quark production has yet to be measured, the limits on this production still test models of physics beyond the Standard Model [12]. Figure 7 illustrates this by comparing the *s*- and *t*-channel limits observed by DØin the neural network analysis against several non-Standard Model contributions. Both the CDF and DØcollaborations continue to refine their multi-variate techniques with the recently available 1 fb^{-1} data samples. Better limits, and perhaps even the discovery of single top-quark production, can be expected in the near future.

Normalization	
$\sigma_{t\bar{t}}$ theory & mass	18%
$\sigma_{s(t)}$ theory	15(16)%
jet fragmentation	5%
lepton ID	5%
Shape and Normalization	
b tag (single/double)	10/20%
JES	10%
trigger	6%
jet identification	5%

Table 3: Systematic uncertainties associated with the DØ neural network analysis.

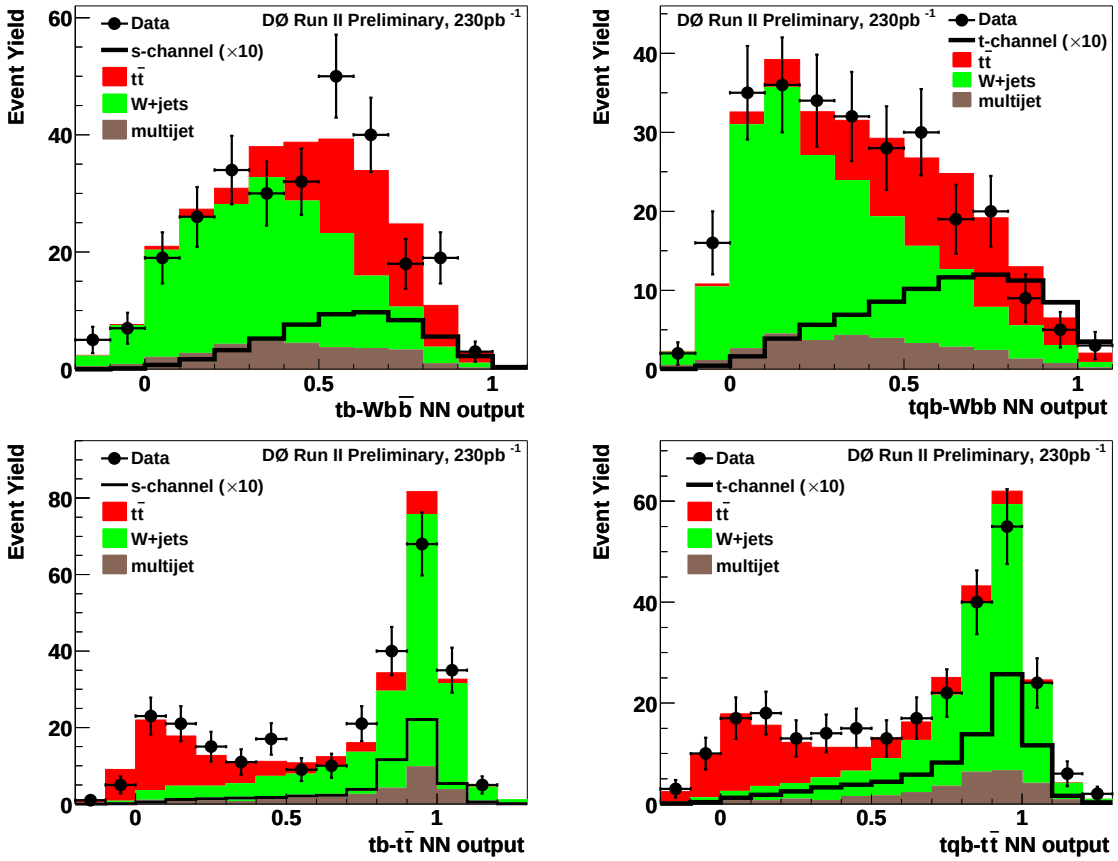

Figure 5: Comparison of background, signal ($\times 10$), and data with at least one b-tagged jet for the neural network outputs. The upper row shows the $Wb\bar{b}$ outputs, the lower row the $t\bar{t}$ outputs. The left column shows the s-channel outputs, the right column the t-channel outputs.

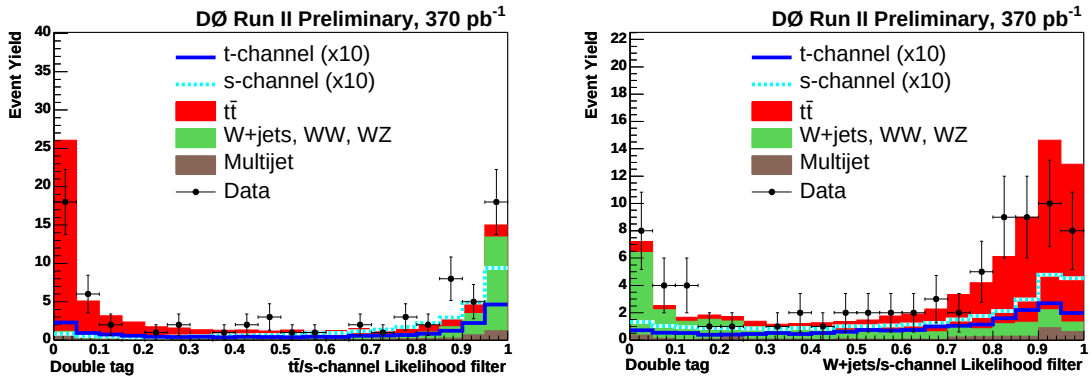

Figure 6: Data to Monte-Carlo comparison for the $tb/t\bar{t}$ (left) and tb/W+jets (right) likelihood discriminant for double-tagged events.

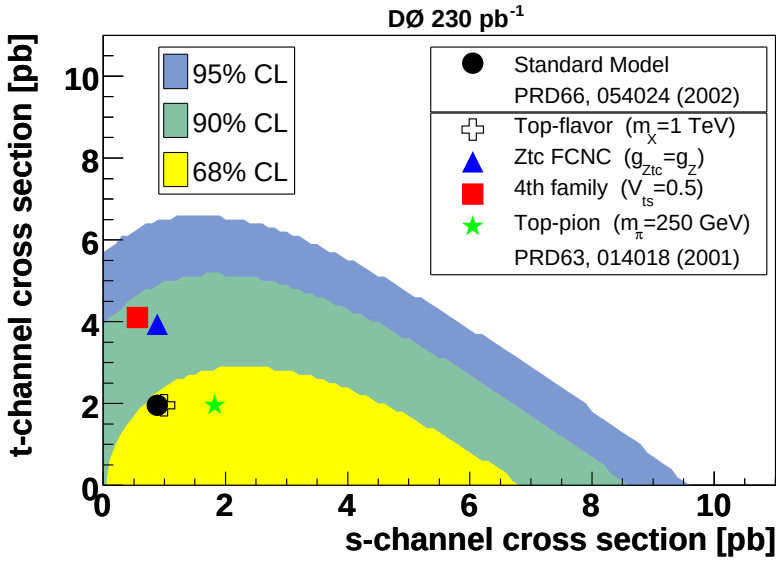

Figure 7: Exclusion contours at the 68%, 90%, and 95% C.L. on the observed posterior density distribution as a function of both the *s*-channel and *t*-channel cross sections in the DØ neural network analysis. Several representative non-Standard Model contributions from Ref. [12] are also shown.

References

[1] F. Abe *et al.* [CDF Collaboration], Phys. Rev. Lett. **74** 2626 (1995);
S. Abachi *et al.* [DØ Collaboration], Phys. Rev. Lett. **74** 2632 (1995).

[2] CDF, DØ, and TEVEWWG Collaborations, hep-ex/0603039.

[3] B. W. Harris *et al.*, Phys. Rev. D **66**, 054024 (2002).

[4] N. Kidonakis and R. Vogt, Phys. Rev. **D68** 114014 (2003); M. Cacciari *et al.*, JHEP **04**068 (2004).

[5] T. Stelzer and W. F. Long, Comput. Phys. Commun. **81**, 337 (1994);
F. Maltoni and T. Stelzer, J. High Energy Phys. **02** (2003) 027.

[6] E. Boos *et al.* [CompHEP Collaboration], Nucl. Instrum. Methods Phys. Res. A **534**, 250 (2004).

[7] T. Sjöstrand *et al.*, Comput. Phys. Commun. **135**, 238 (2001).

[8] M. L. Mangano *et al.*, JHEP **0307**, 001 (2003).

[9] D. Acosta *et al.* [CDF Collaboration], Phys. Rev. D **71**, 012005 (2005).

[10] V. M. Abazov *et al.* [DØ Collaboration], Phys. Lett. B **622**, 265 (2005).

[11] Y. Coadou, these proceedings.

[12] T. Tait and C. P. Yuan, Phys. Rev. D **63**, 014018 (2001).